

**JOINING OF ALUMINA-BASED COMPOSITE TO 6061 ALUMINUM
ALLOY BY FRICTION WELDING**

by

MARJAN SAFARZADEH

**Thesis submitted in fulfillment of the
requirements for the degree of
Master of Science**

June 2014

ACKNOWLEDGMENTS

Foremost, I would like to express my sincere gratitude to my supervisor Prof. Dr. Ahmad Fauzi Mohd Noor for his continuous support, patience, motivation, enthusiasm, and immense knowledge in the completion of this thesis. Without his reading, guidance, corrections and re-reading my drafts this thesis would never have been completed.

My sincere thanks also go to the Dean, Deputy Dean, lecturers and technicians of the School of Material and Mineral Resources Engineering of USM for providing me with all the necessary facilities and put my mind at ease.

I wish to express my deepest gratitude to my parents for their unceasing encouragement and supporting financially and spiritually throughout my life.

I am grateful to my dear friend Dr. Reza Mohammadpour Ghalati for his great help and all he did throughout writing my thesis.

I would like to thank Dr. Uday, M.B. (my senior) for his advices while doing this research.

MARJAN SAFARZADEH

TABLE OF CONTENTS

| | |
|---|-----|
| ACKNOWLEDGMENTS | ii |
| TABLE OF CONTENTS | iii |
| LIST OF TABLES..... | vi |
| LIST OF FIGURES | vii |
| LIST OF SYMBOLS..... | xii |
| ABSTRAK | xv |
| ABSTRACT | xvi |
| CHAPTER 1 - INTRODUCTION | |
| 1.1 Overview | 1 |
| 1.2 Problem statement..... | 4 |
| 1.3 Objectives of the research | 6 |
| 1.4 Research approach | 7 |
| CHAPTER 2 - LITERATURE REVIEW | |
| 2.1 Friction welding | 8 |
| 2.2 Principle of friction welding | 9 |
| 2.3 History of friction welding..... | 9 |
| 2.4 Mechanism of friction welding | 10 |
| 2.5 Friction welding parameters..... | 12 |
| 2.5.1 Time..... | 12 |
| 2.5.2 Speed | 13 |
| 2.5.3 Pressure | 13 |
| 2.6 Interface temperature | 14 |
| 2.7 Heat generation | 15 |
| 2.8 Structure of the heat affected zone (HAZ)..... | 17 |
| 2.9 Classification of friction welding process..... | 18 |
| 2.9.1 Rotary friction welding | 18 |
| 2.9.2 Friction stir welding | 23 |

| | | |
|--------|---|----|
| 2.10 | Types of relative motion in friction welding..... | 25 |
| 2.11 | Friction welding for similar and dissimilar materials | 27 |
| 2.12 | Friction welding of metals | 28 |
| 2.12.1 | Friction welding of Aluminium alloys | 28 |
| 2.12.2 | Friction welding of aluminium alloys with other metals ... | 30 |
| 2.13 | Friction welding of ceramics..... | 33 |
| 2.13.1 | Friction welding of ceramics with aluminium alloys..... | 35 |
| 2.14 | Advantages and shortcomings of friction welding Process | 39 |
| 2.15 | Process applications | 41 |
| 2.16 | Summary | 41 |

CHAPTER 3 - MATERIALS AND METHODOLOGY

| | | |
|--------|--|----|
| 3.1 | Introduction..... | 42 |
| 3.2 | Raw materials..... | 42 |
| 3.2.1 | 6061 Aluminum alloy..... | 42 |
| 3.2.2 | Ceramic materials..... | 42 |
| 3.2.3 | PVA..... | 43 |
| 3.3 | Sample preparation for friction welding | 43 |
| 3.3.1 | Preparation of 6061 Aluminum alloy specimens | 45 |
| 3.3.2 | Fabrication of alumina specimens..... | 46 |
| 3.3.3 | Preparing mullite sample rods..... | 50 |
| 3.4 | Friction welding process | 51 |
| 3.5 | Characterization | 54 |
| 3.5.1 | X-Ray Fluorescence (XRF) Analysis..... | 54 |
| 3.5.2 | X-Ray Diffraction (XRD) Analysis | 55 |
| 3.5.3 | Particle-Size Distribution (PSD) | 56 |
| 3.5.4 | Field Emission Scanning Electron Microscopy (FESEM).56 | |
| 3.5.5 | Energy Dispersive X-Ray (EDX)..... | 57 |
| 3.5.6 | Fractography..... | 58 |
| 3.5.7 | Optical microscopy (OM) | 58 |
| 3.5.8 | Density and Porosity | 58 |
| 3.5.9 | Linear shrinkage | 59 |
| 3.5.10 | Three point bending strength..... | 60 |
| 3.5.11 | Four point bending strength | 62 |

| | |
|-----------------------------------|----|
| 3.5.12 Vickers Microhardness..... | 63 |
|-----------------------------------|----|

CHAPTER 4 - RESULT AND DISCUSSION

| | | |
|-------|---|-----|
| 4.1 | Introduction..... | 65 |
| 4.2 | Raw materials characterization | 65 |
| 4.2.1 | X-Ray Fluorescence (XRF) Analysis..... | 65 |
| 4.2.2 | X-Ray Diffraction (XRD) Analysis | 66 |
| 4.2.3 | Particle Size Distribution analysis (PSD)..... | 68 |
| 4.2.4 | Field Emission Scanning Electron Microscopy (FESEM).68 | |
| 4.3 | Fabrication of ceramic specimens for friction welding..... | 71 |
| 4.3.1 | Sintering of Alumina rod..... | 72 |
| 4.3.2 | Mullite rod by reaction sintering SiO ₂ and Al ₂ O ₃ | 75 |
| 4.3.3 | Mullite rod from commercial mullite powder..... | 87 |
| 4.3.4 | Composite of Alumina-Mullite rods | 94 |
| 4.4 | Three point bending strength | 101 |
| 4.5 | Friction welding of Al ₂ O ₃ to 6061 Al-alloy | 101 |
| 4.5.1 | Microstructure of Friction Welding between Al ₂ O ₃ and 6061 Al-alloy..... | 102 |
| 4.5.2 | Mechanical Properties of Friction Welding Al ₂ O ₃ / 6061 Al-alloy | 110 |
| 4.6 | Friction welding of Mullite and 6061 Al-alloy | 112 |
| 4.7 | Friction welding of Alumina-Mullite Composite and 6061 Al-alloy | 114 |
| 4.7.1 | Microstructure of Friction Welding joint between Alumina-Mullite Composite and 6061 Al-alloy..... | 115 |
| 4.7.2 | Mechanical Properties of Friction welding Alumina-Mullite composite with 6061 Al-alloy | 128 |

CHAPTER 5 - CONCLUSION AND RECOMMENDATION

| | | |
|-----|--|-----|
| 5.1 | Conclusions..... | 134 |
| 5.2 | Recommendation for future research | 135 |

| | |
|-------------------------|-----|
| REFERENCES | 136 |
|-------------------------|-----|

APPENDICES

LIST OF TABLES

| | | |
|-------------|--|-----|
| Table 2.1: | Friction weld ability of aluminium and aluminium alloys to other metals (Kato and Tokisue, 2004) | 32 |
| Table 4.1: | The chemical composition of 6061 Al-alloy by XRF technique | 66 |
| Table 4.2: | The Chemical composition of raw ceramic powders by XRF technique | 66 |
| Table 4.3: | Particle size distribution | 68 |
| Table 4.4: | The rheological properties of alumina slip | 73 |
| Table 4.5: | The properties of sintered Alumina rods | 73 |
| Table 4.6: | The rheological properties of alumina-silica slip | 75 |
| Table 4.7: | The properties of alumina-silica samples | 77 |
| Table 4.8: | The rheological properties of mullite slip | 87 |
| Table 4.9: | The properties of sintered mullite samples at various temperatures | 89 |
| Table 4.10: | The rheological properties of composite Alumina-Mullite slip | 95 |
| Table 4.11: | The properties of Alumina- Mullite composite samples | 97 |
| Table 4.12: | The average three point bending strength of the ceramic rods | 101 |
| Table 4.13: | Four point bending strength of Alumina /6061 Al-alloy welded interface at 1250 rpm | 112 |
| Table 4.14: | Mechanical properties of mullite and alumina ceramics (Schneider et al., 2008) | 112 |

LIST OF FIGURES

| | | |
|--------------|--|----|
| Figure 2.1: | Basic steps in friction welding (Kalsi & Sharma, 2011) | 11 |
| Figure 2.2: | Schematic illustration of the different regions in the HAZ of friction welded specimens; (i) full plastic deformed zone (FPDZ); (ii) deformed zone (DZ); (iii) undeformed zone (UZ) (Ahmad Fauzi et al., 2010) | 18 |
| Figure 2.3: | Schematic representation of the rotary manner | 19 |
| Figure 2.4: | Schematic setup of a direct drive-welding machine (Davari et al., 2011) | 21 |
| Figure 2.5: | Schematic of parameter variations for direct drive friction welding process (Maalekian, 2007) | 21 |
| Figure 2.6: | Schematic setup of an inertia-welding machine (Davari et al., 2011) | 22 |
| Figure 2.7: | Schematic of parameter variations for inertia friction welding process (Maalekian, 2007) | 23 |
| Figure 2.8: | Schematic illustration of friction stirs welding (Nandan et al., 2008) | 25 |
| Figure 2.9: | Schematic of typical arrangement of rotational friction welding a) Basic, b) Counter rotation, c) Centre drive (splicing), d) Twin welds, e) Centre drive (dual production) (Messler, 2008) | 26 |
| Figure 2.10: | Schematic of shape and dimension of specimen used for friction welding (Kanayama et al., 1985) | 36 |
| Figure 2.11: | Cross-section views of friction zone welded by, (a) flat ceramic face to flat metal face, (b) taper pin angle 60° ceramic face to flat metal face, (c) taper pin angle 30° ceramic face to flat metal face, (d) pin ceramic face to flat metal face (Uday and Ahmad Fauzi, 2013) | 38 |
| Figure 3.1: | Flowchart of ceramic and 6061 Al-alloy preparation and friction welding | 44 |
| Figure 3.2: | The dimension of the aluminum alloy specimens | 45 |
| Figure 3.3: | Schematic process of slip casting (Boch & Nièpce, 2010) | 48 |

| | | |
|--------------|--|----|
| Figure 3.4: | The dimension of alumina sample pre-sintered at 1200°C and sintered at 1600°C respectively | 48 |
| Figure 3.5: | Schematic profile of shrinkage at a) pre-sintering and b) final sintering | 49 |
| Figure 3.6: | Schematic diagram of pre-sintering profile of ceramic sample | 49 |
| Figure 3.7: | Schematic diagram of final sintering profile of ceramic sample | 50 |
| Figure 3.8: | A modified lathe machine with hydraulic press used for friction welding | 53 |
| Figure 3.9: | Rotary and stationary jaw used in friction welding machine | 54 |
| Figure 3.10: | a) Test layout for the three point bending test b) Schematic diagram of three point bending test | 61 |
| Figure 3.11: | a) Test layout for the four point bending test b) Schematic diagram of four point bending test | 63 |
| Figure 3.12 | The welded sample which was cut and polished | 64 |
| Figure 4.1: | The XRD pattern of raw materials, mullite, silica, alumina, aluminum | 67 |
| Figure 4.2: | FESEM Micrograph of a) 6061 Al-alloy grains etched in 1% NaOH solution for 15 min b) alumina powder c) silica powder d) mullite powder | 69 |
| Figure 4.3: | FESEM Micrograph of sintered Alumina at 1600°C | 74 |
| Figure 4.4: | The XRD pattern of the alumina-silica forming mullite after sintering at 1200, 1550 and 1600°C for 2hr. | 76 |
| Figure 4.5: | FESEM Micrograph of polished surface of alumina-silica forming mullite sintered at a)1200°C b)1550°C c)1600°C for 2hr. Etched at 0.5%HF 1min.Heating and cooling rate 5°Cmin-1 [magnification 3000] | 78 |
| Figure 4.6: | FESEM Micrograph of the fracture surface of alumina-silica forming mullite sintered at a)1200°C b)1550°C c)1600°C for 2hr. Heating and cooling rate 5°Cmin-1 [magnification 3000] | 79 |
| Figure 4.7: | EDX of alumina-silica forming mullite sintered at 1200°C for 2hr at (a) for particle A, (b) for particle B, and (c) for particle C. Heating and cooling rate 5°Cmin-1 | 80 |

| | | |
|--------------|---|-----|
| Figure 4.8: | EDX of alumina-silica forming mullite sintered at 1550°C for 2hr at (a) for particle A, (b) for particle B, and (c) for particle C. Heating and cooling rate 5°Cmin-1 | 82 |
| Figure 4.9: | EDX of alumina-silica forming mullite sintered at 1200°C for 2hr at (a) for particle A, (b) for particle B, and (c) for particle C. Heating and cooling rate 5°Cmin-1 | 84 |
| Figure 4.10: | FESEM of crack on alumina-silica forming mullite sintered at a) 1200°C b) 1600°C for 2 h. Heating and cooling rate 5°Cmin-1 [magnification 100] | 86 |
| Figure 4.11: | Optical images of crack on alumina-silica forming mullite sintered at 1200°C for 2hr. Heating and cooling rate 5°Cmin-1 [magnification 100] | 86 |
| Figure 4.12: | The XRD pattern of the mullite specimen sintered at 1500, 1550, 1600 and 1650°C for 2hr. | 88 |
| Figure 4.13: | FESEM microstructure of polished mullite samples sintered at a) 1200, b) 1500, c) 1550 and d) 1600 for 2hr .Heating rate 5°Cmin-1. Etched at 0.5%HF 1min [magnification 5000] | 91 |
| Figure 4.14: | FESEM microstructure of fractured surface of the mullite samples sintered at a) 1200, b) 1500, c) 1550 and d) 1600 e) 1650°C for 2hr .Heating rate 5°Cmin-1. Etched at 0.5%HF 1min [magnification 5000]. | 93 |
| Figure 4.15: | The XRD pattern of Alumina-Mullite composite sintered at 1200°C and 1600°C for 2hr. Heating and cooling rate 5°Cmin-1. | 96 |
| Figure 4.16: | FESEM microstructure of polished Alumina-Mullite composite sample sintered at a) 1200°C, b) 1600°C for 2hr. Heating and cooling rate 5°Cmin-1. [magnification 5000]. | 98 |
| Figure 4.17: | FESEM microstructure of fracture Alumina-Mullite composite sample sintered at a) 1200°C, b) 1600°C for 2hr. Heating and cooling rate 5°Cmin-1. [magnification 5000] | 99 |
| Figure 4.18: | EDX of Alumina-Mullite composite sintered at a) 1200°C at point A, b) 1600°C at point B ,for 2hr. Heating and cooling rate 5°Cmin-1 | 100 |
| Figure 4.19: | The optical images of Alumina/6061 Al-alloy welded interface properties a) 50 , b) 100 | 103 |

| | | |
|--------------|--|-----|
| Figure 4.20: | FESEM of Alumina/6061 Al-alloy welded interface properties at 1250 rpm after etching in 1% NaOH, time: 15min [magnification a)500 , b) 1000] | 105 |
| Figure 4.21: | EDX of Alumina/ 6061Al-alloy welded interface at 1250 rpm after etching in 1% NaOH, time: 15min at a) point A, b) point B and c) point C | 106 |
| Figure 4.22: | FESEM fractography of Alumina/ 6061Al-alloy joint at 1250 rpm at [magnification a) 1000 , b) 3000] | 109 |
| Figure 4.23: | Microhardness of friction welded Alumina/6061 Al-alloy at 1250 rpm | 110 |
| Figure 4.24: | FESEM fractography of Mullite/ 6061 Al-alloy welded interface at 1250 rpm at [magnification a) 1000 , b) 3000] | 114 |
| Figure 4.25: | The optical images of Alumina- Mullite Composite / 6061 Al-alloy welded interface properties at 1250 rpm a) 50 , b) 100 | 116 |
| Figure 4.26: | The optical images of Alumina- Mullite Composite / 6061 Al-alloy welded interface properties at 1800rpm a) 50 , b) 100 | 117 |
| Figure 4.27: | FESEM of Alumina-Mullite composite /6061 Al-alloy welded interface properties at 1250 rpm after etching in 1% NaOH, time: 15min [magnification a) 1000 , b) 3000] | 119 |
| Figure 4.28: | FESEM of Alumina-Mullite composite /6061 Al-alloy welded interface properties at 1800 rpm after etching in 1% NaOH, time: 15min [magnification a) 1000 , b) 3000] | 120 |
| Figure 4.29: | EDX of Alumina-Mullite composite with 6061 Al-alloy welded interface at 1250 rpm after etching in 1% NaOH, time:15min at a) point A, b) point B, c) point C | 121 |
| Figure 4.30: | EDX of Alumina-Mullite composite with 6061 Al-alloy welded interface at 1800 rpm after etching in 1% NaOH, time: 15min at a) point A, b) point B, c) point C | 123 |
| Figure 4.32: | FESEM fractography of Alumina-Mullite composite (Al-M) /6061 Al-alloy joint at rotational speed 1800 rpm after four point bending test [magnification a) 500 , b) 1000] | 127 |

| | | |
|--------------|---|-----|
| Figure 4.33: | Microhardness traverse of friction welded Alumina-Mullite composite/6061 Al-alloy at 1250 rpm | 129 |
| Figure 4.34: | Microhardness traverse of friction welded Alumina-Mullite composite/6061 Al-alloy at 1800 rpm | 130 |
| Figure 4.35: | Four point bending strength of friction welded Alumina-Mullite composite / 6061 Al-alloy | 131 |
| Figure 4.36: | Appearance of friction welded alumina, mullite and Alumina-Mullite composite with 6061 Al-alloy after four point bending strength with different rotating speed | 133 |
| Figure A.1: | The distribution particle size of a) Mullite b) Silica and c) Alumina | |

LIST OF SYMBOLS

| Symbol | Description |
|-------------------|---|
| a | Distance between an inner loading point and an outer support point (mm) |
| d | Arithmetic mean of the two diagonal length (mm) |
| D | Diameter (mm) |
| D_0 | Diameter before sintering (mm) |
| D_f | Diameter after sintering (mm) |
| D_s | Percentage of shrinkage in diameter (mm) |
| F | Applied force (N) |
| H_v | Vickers hardness(N/mm ²) |
| K_{Ic} | Fracture toughness (MPa m ^{0.5}) |
| L | Length (mm) |
| L_0 | Outer support span (mm) |
| L_i | Inner support span (mm) |
| $Wt \%$ | Weight percent |
| W_d | Weight of dry sample (g) |
| W_s | Weight of the suspended sample in distilled water (g) |
| W_m | Weight of the saturated sample (g) |
| ρ | Bulk density (g/cm ³) |
| σ | Strength, MPa |
| μm | Micrometer |
| $\Omega \cdot cm$ | Ohm.cm |

LIST OF ABBREVIATION

| Abbreviation | Description |
|--|---|
| 6061 Al-alloy | Precipitation hardening aluminum alloy |
| Al ₂ O ₃ | Aluminum Oxide |
| 3Al ₂ O ₃ .2SiO ₂ | Mullite |
| AWS | American Welding Society |
| BSE | Back Scattered Electron |
| CDFW | Continuous drive friction welding |
| CTE | Coefficient of Thermal Expansion |
| DZ | Deformed Zone |
| EDX | Energy Dispersive X-ray Spectroscopy |
| FESEM | Field Emission Scanning Electron Microscope |
| FPDZ | Full Plastic Deformed Zone |
| FSW | Friction Stir Welding |
| FW | Friction Welding |
| HAZ | Heat Affected Zone |
| HF | Hydrofluoric Acid |
| IFW | Inertia friction welding |
| NaOH | Sodium hydroxide |
| OM | Optical microscopy |
| PSD | Particle Size Distribution |
| pH | Concentration of hydrogen's ion |

| | |
|------------------|----------------------------------|
| POP | Plaster of Paris |
| PVA | Poly vinyl alcohol |
| RFW | Rotary Friction Welding |
| SE | Secondary Electrons |
| SiO ₂ | Silicon dioxide |
| TMAZ | Thermomechanically Affected Zone |
| TWI | The Welding Institute |
| UZ | Unaffected Zone |
| XRD | X-ray Diffraction |
| XRF | X-ray Fluorescence |

PENYAMBUNGAN ALUMINA BERASASKAN KOMPOSIT DENGAN 6061 ALOI ALUMINIUM MELALUI KIMPALAN GESERAN

ABSTRAK

Kajian ini bertujuan untuk menilai kemampuan kimpalan geseran ke atas komposit mulit dan Alumina-Mulit dengan aloi-Al 6061, serta seterusnya menentukan sifat-sifat mikrostruktur dan mekanikal. Semasa proses ini, daya geseran (1000 bar) dan masa geseran (30 Saat) telah ditetapkan manakala kelajuan putaran berubah. Rod seramik telah disediakan melalui penuangan slip, diikuti pra-sinter pada 1200°C dan disinter pada 1600°C dengan kadar pembakaran dan penyejukan pada 5°C/min, manakala rod aluminium telah dimesin untuk mendapatkan dimensi sesuai dan kemudian digilap. Kelakuan pensinteran sampel seramik telah disiasat. Kesimpulannya, rod mulit tidak mampu disambung dengan aloi-Al 6061 kerana mulit mempunyai ketahanan patah yang rendah. Oleh itu, ketahanan patah telah dipertingkatkan melalui komposit Alumina-mulit. Proses kimpalan telah dilaksanakan dengan dua kelajuan putaran yang berbeza (1250 dan 1800 rpm). Tambahan pula, kesan peningkatan kelajuan putaran terhadap mikrostruktur, kekerasan-mikro dan sifat mekanikal sambungan Alumina-Mulit komposit /aloi-Al 6061 telah dinilai. Didapati mikrostruktur, kekerasan-mikro dan sifat-sifat mekanik yang baik telah dicapai melalui sambungan komposit Alumina-mulit dengan aloi-Al 6061 pada kelajuan putaran yang lebih tinggi (1800 rpm). Mekanisme kegagalan pada permukaan patah mendedahkan ciri hasil yang berbeza pada kelajuan yang berbeza. Pada kelajuan yang lebih tinggi ciri lesung pipit dan mulur dibentuk yang membayangkan ubah bentuk plastik berlaku.

JOINING OF ALUMINA-BASED COMPOSITE TO 6061 ALUMINUM ALLOY BY FRICTION WELDING

ABSTRACT

The present research is aimed at evaluating the feasibility of using the friction welding of mullite and Alumina-Mullite composite with 6061 Al-alloy, and subsequently determining their microstructural and mechanical properties. During the process, friction force (1000 bar) and friction time (30 Sec) were held constant while the rotational speed was varied. Ceramic rods were prepared through slip casting, subsequently pre-sintered at 1200°C and sintered at 1600°C with heating and cooling rate 5°C/min, while the aluminium rods were machined down to get the require dimension and then polished. Sintering behaviour of ceramic samples were investigated. It was concluded that the mullite rods didn't join to 6061 Al-alloy due to the low fracture toughness of the mullite. Thus, fracture toughness was improved through the composite of Alumina-Mullite. Welding process was carried out under two different rotational speeds (1250 and 1800rpm) and the effect of increasing rotational speed on microstructure, microhardness and mechanical properties of Alumina-Mullite composite/6061 Al-alloy joined was evaluated. It was observed that a good microstructure with higher mechanical properties (microhardness and bending strength) were achieved from the joining of Alumina-Mullite composite with 6061 Al-alloy at higher rotational speed (1800 rpm). The mechanisms of failure at the fracture surfaces revealed different feature at different speed. At the higher speed dimple and ductile formed which implies the plastic deformation.

CHAPTER1

INTRODUCTION

1.1 Overview

Ceramic-metal joints have become more significant in modern technology, due to the combination of the properties of metals like ductility, high electrical and thermal conductivity and the properties of ceramics such as high hardness, corrosion and wear resistance (Noh et al., 2008; Uday and Ahmad Fauzi, 2013). With respect to this, the microstructural development on ceramic–metal interfaces plays a critical role for these processes to be successful. The evolution of interface formation of ceramic-metal is not simple and requires the study on thermodynamics, kinetics, and mechanical properties of all of the phases that are present (Meier et al., 1999; Noh et al., 2008).

Friction Welding is a solid-state joining that produces coalescence at the faying surfaces under the compressive force involving one rotating and one stationary component. The coalescence of the materials will be obtained through the combination of a mechanically induced pressure and the rubbing motion of the two components (Jesudoss Hynes et al., 2013). Subsequently mechanical energy directly converts to the thermal energy at the interface of the components. Eventually heat generates at the joint interface would induce plastic deformation of the material and then forms upset. When certain amount of forging had occurred, the rotation stopped and the compressive force was maintained or slightly increased to consolidate the weld. This

process is also associated with physical phenomena such as frictional heat generation, plastic deformation, cooling of high-temperature metal and the solid state phase variation (Celik and Gunes, 2012; Jesudoss Hynes et al., 2013).

Uday et al. (2013) had studied the effect of friction time, heating time and the rotational speed on the microstructure and mechanical properties. They carried out the welding process of alumina with 0, 25, 50 wt% yttria stabilized zirconia (YSZ) composite to 6061 aluminium alloy under different rotational speeds and friction times, while friction force (0.5 ton-force) was held constant. The results showed that the friction temperature at a higher friction time (90 sec) increased the formation of brittle phases as well as thermal expansion between the metal–ceramic. Consequently, the value of bending strength was lower when compared to lower friction time (30 sec).

Similarly, the effects of friction time and friction pressure on strength of aluminium and copper joints using statistical analysis was carried out by Sahin (2010). The strength of joints was determined by tensile tests. The results revealed that as the friction time and pressure for the joints was increased, tensile strength of the joints increased to an optimum, then decreased with further increase in friction time and pressure. Some of the results showed poor tensile strength for Cu–Al joints because of the formation intermetallic compounds at the interface but compared with those of the base metals, the results were acceptable.

Kurt et al. (2011) examined the effect of friction welding parameters on mechanical properties and optimal welding of ASTM B22 Tin bronze and AISI 1010 joints. Generally, the hardness values increased with increasing friction pressure and upset pressures, but hardness values decreased with increasing upset time. Increasing hardness in the welding interface was attributed to the diffusion of elements on the sides as a result of the heat input and plastic deformation.

The rotational speed is related to the materials being joined or more specifically, the mechanical and physical properties involved, and also the diameter of the weld at the interface. High rotational speeds might generate greater heat at the interface, which leads to softening of the metal, consequently greater extent of recrystallization, or even increased intermetallic formation (Yeoh et al., 2004). As a result, appropriate rotational speed is needed to minimize any detrimental effects and produce joints of good quality.

Heating time is determined during the set-up or from previous experience. Heating time must be carefully controlled to avoid overheating of the weld zone and possible cracking during cooling. Excessive heating would limit output and increase waste material. On the other hand, uneven heating would entrapped oxides, caused unbounded region at the interface which is attributed to the insufficient welding time (Narayana et al., 2006; khan,2012).

The effective pressure ranges are also broad for heating and forging although the selected pressure should be reproducible for any specific operation. The pressure controls the temperature gradient in the weld zone, the required drive power and the axial shortening (Connor et al., 1987; Gowri, 2007; Khan, 2012).

1.2 Problem statement

The friction welding of dissimilar materials somewhat is more complicated when comparing to welding of similar materials and this is because of the differences in physical, mechanical, chemical and thermal properties (Satyanarayan et al., 2003; Uday & Ahmad Fauzi, 2013). In the case of ceramic–metal, the interface of the joints is a critical aspect in the joining and processing of these interfaces is fundamental to fabrication of a wide range of materials and devices. The application of the advanced ceramics depends on the reliability of ceramic-metal joining processes and also the properties of the resulting interfaces (Lemus Ruiz et al., 2008).

Joint strength have been associated with several condition which if not controlled, would influenced the consistency of a joint, such as formation of the intermetallic layer which are responsible for brittle failure of the components. On the other hand the mismatch in coefficient of thermal expansion, CTE, of the joining materials can result in high residual stresses at the interface during cooling (Lemus Ruiz et al., 2008). To control the formation of the intermetallic layer, the friction time and speed should be control. To overcome the mismatch in CTE, the ceramic and metallic

components should be selected with minimal thermal expansion differences throughout their operation range.

The main goal for joining is to produce a strongly bond interface by eliminating defects and by accommodating thermal stresses. These residual stresses reduce the strength of the bonded material and in some cases lead to joint failure during or after the joining process. Thus, for understanding the mechanical performance of the welded joints, studying the mechanisms of interface formation between the metal and ceramic is very important (Lemus Ruiz et al., 2008).

Consequently, this research is focused on the fabrication and characterization of alumina, mullite and Alumina-Mullite composite and subsequently joining of them with 6061 Al-alloy by friction welding process. The main reason for these selected materials is to produce a novel metal alloy-ceramic composite joining by friction welding technique, which also provides a new data analysis system for future research.

The 6061 Al-alloy was chosen for this study due to the moderate strength, good toughness, high corrosion resistance, low density, good forming and processing properties. It has been widely applied in areas of aerospace, marine structures, automobile industries and modern architecture (Mishra and Mahoney, 2006). The 6061 Al alloy is the most popular aluminum alloy extrusion. In recent years, with the verification of modern manufacture methods and the complications of product structures, it becomes

important to join the similar and dissimilar materials with different states in practical applications.

Mullite was chosen as a ceramic part because it has been considered to be an important material for advanced structural applications owing to its unique combination of properties such as good mechanical strength, good thermal shock resistance, high creep resistance, low thermal expansion, as well as good chemical and thermal stability (Wang et al., 2010). Major activities have been focussed on continuous fiber-reinforced mullite matrix composites, especially using alumina and mullite fibers. Important application fields of such composites are components and structures for gas turbine engines (liners, thermal protection shingles for combustors, exhaust cones), high duty kiln furnitures, burner tubes, and heat shields for re-entry space vehicles (Schneider et al., 2008).

However, due to poor joining abilities of mullite, the Alumina-Mullite composite containing 70wt% alumina and 30wt % mullite were prepared. The composite would have improve toughness, which enhance joining ability.

1.3 Objectives of the research

The main objectives of this research are as follows:

1. Investigate the possibility of friction welding of alumina, mullite and Alumina-Mullite composite with 6061 Al-alloy
2. Characterization and evaluation of the microstructural and mechanical properties at the joint interface of friction welded samples.

1.4 Research approach

This research is divided into two stages; firstly the sample preparation, and secondly the joining process. The first stage contains preparing alumina, mullite and Alumina-Mullite composite through slip casting and cutting 6061 Al-alloy rods into require diameters and polishing. The second stage is the attempt to friction welding the ceramic rods to 6061 Al-alloy rods. In chapter 3, Figure 3.1 shows the various stages in the research. After friction welding, the mechanical properties, as well as plastic deformation and joint microstructure were investigated.

CHAPTER2

LITERATURE REVIEW

2.1 Friction welding

Mostly joining different materials or dissimilar materials is not an easy task, because atoms, ions or molecules in ceramics, metals or polymers of different classes, joined together in different ways, and thus characterized by particular combinations properties such as physical, chemical as well as mechanical. Accordingly, for joining dissimilar materials, property mismatches should be accounted and minimized (Nascimento et al., 2003).

Different techniques have been used for joining ceramic–metal and these include among others as ultrasonic joining, brazing, transient liquid phase, diffusion bonding and FW (Nascimento et al., 2003; Jesudoss Hynes et al., 2013). However, these methods have lower efficiency in compare with friction welding (Ahmad Fauzi et al., 2010).

Friction welding (FW) method is one of the most economical and productive methods for joining of similar and dissimilar materials, which provides the advantage of high joint integrity (Uday and Ahmad Fauzi, 2013). During this process, heat is generated by conversion of mechanical energy into thermal energy at the interface of the work pieces during rotation under pressure. Some advantages of the friction welding are low material waste, short production time and welding of parts of different metals or alloys are

made possible. Friction welding can also be used in joining of components that have circular or non- circular cross-sections (Sahin, 2005).

2.2 Principle of friction welding

Friction welding (FW) is a solid-state joining process in which the coalescence of materials is produced by generating heat between surfaces through the combination of a mechanically induced rubbing motion and the applied load. The resulting joints are of forged quality. Under normal conditions, the contact surfaces during FW do not melt but soften (meaning the metal is not melted during the process) (Nguyen and Weckman, 2006; Maalekian, 2007; Akbarimousavi and Goharikia, 2011; Winiczenko and Kaczorowski, 2013; Uday et al., 2013). The friction welding process requires a machine which is designed to convert mechanical energy into heat at the joint interface using relative movement between components.

2.3 History of friction welding

Friction welding as a method of joining was first revealed in the 1891's by Bevington who found the possibility for use of friction to generate heat for both welding and forming (Nicholas, 2003). From the 1930's to 1940's, 'spin welding' of plastics was developed (Mistry, 1997). The use of friction for welding increased in the 1950's. On a more worldwide scale, the process gained acceptability for high volume production and its ability to join a wide range of material in similar and dissimilar materials.

Generally, changes were to come in the mid 70's when orbital and linear reciprocating motions appeared which then enabled the joining of non-round parts with accurate angular alignment. Another major milestone reached in 1991 when Wayne Thomas of TWI invented friction stir welding (Nicholas, 2003).

2.4 Mechanism of friction welding

In friction welding, a joint between two specimens can be formed through the rubbing motion by compressive force when one component is rotating and one is stationary (Woo et al., 2002; Lee et al., 2003; Uday, 2013). Subsequently due to the continuous rubbing of faying surfaces heat is generated, which in turn, causes softening of material and eventually plastically displacing the material from the faying interface generated. Ultimately, the heated material at the faying interface will tend to upset, resulting in plastic flow (Nguyen and Weckman, 2006; Maalekian, 2007; Uday et al., 2013). Finally, the friction welding process is completed by stopping the rotation and maintaining or slightly increasing a high compressive force after a certain amount of upset has occurred to consolidate the weld (Akbarimousavi and Goharikia, 2011).

Hasui and Fukushima (1977) concluded that the welding cycle could be divided into four stages. Figure 2.1 shows the steps for friction welding process. The process can be well explained in four stages. Initially one component is kept stationary while another one is rotating. As shown in Figure 2.1(a) rotating component is brought up to desire speed. Figure 2.1(b)

shows the non rotating component advanced to meet the rotating component and pressure is applied. As shown in Figure 2.1(c), pressure and rotation was maintained for a specified time. Meanwhile, heat generated at the interface due to the continuous rubbing and began to form upsets. Finally rotation of the component was stopped and pressure either maintained or slightly increased (Figure 2.1(d)) (Kalsi and Sharma, 2011).

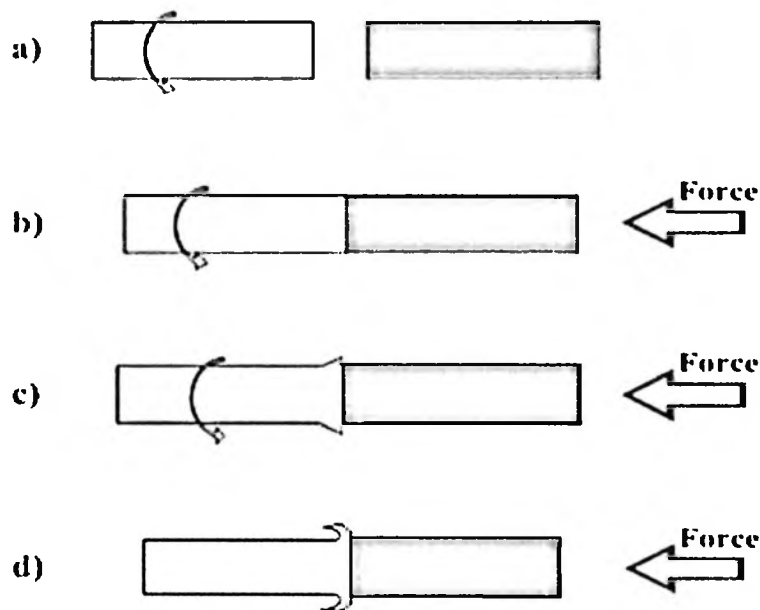


Figure 2.1: Basic steps in friction welding (Kalsi & Sharma, 2011)

According to Maalekian (2007) in general friction welding involves three basic stage; Heat-up stage, burn-off stage and forging stage. During the first stage (heat-up stage), the two components, are brought into contact which have relative motion against each other, and an axial compressive force is applied. Heat is generated, as the faying surfaces (weld interface) rub together, interface temperature is raised by continuously rubbing which cause

decrease in the flow stress of the material. Ultimately, the material is unable to resist the applied axial compressive force and plastically flow expelled to the outside as flash. Flash formation takes place during the burn-off stage. Eventually, in the forging stage, the welding process is completed by ceasing the relative motion and applying a high axial force.

2.5 Friction welding parameters

The fundamental parameters of friction welding (FW) are time, speed and pressure. These factors control the characteristics of a weld to obtain a uniform and strong joint (Maalekian, 2007; Uday et al., 2011a). In other words, the selection of the welding parameters influences the microstructure (Sathiya et al., 2007). The details of the parameters are discussed in the following section.

2.5.1 Time

Friction time would be one parameter influencing the welding process. Friction time is directly related to material properties. Since the heating time in friction welding is short, it suggests that the joint is formed during cooling due to the relatively long cooling period (Maalekian, 2007). The friction time should allow plastic deformation to take place or remove possible residuals (Uzkut et al., 2010). At high friction time, a broad diffusion zone with intermetallic phases can be generated. On the other hand, very low friction time can cause non-uniform heating which result in inadequate plastic deformation and consequently poor joining region at the interface. To achieve higher strength, the friction time should be kept as short as possible, while the

friction and upsetting pressures should be as high as possible (Sathiya et al., 2007).

2.5.2 Speed

The speed of rotation is normally expressed by the circumferential speed at the outer diameter of the cylindrical speed (Bonte et al., 2010). Variation in rotational speeds may lead to different effects on the mechanical properties of friction joints. Increasing rotational speed may generate greater heat at the faying interface, hence resulting in softening of the material, a greater extent of recrystallization and even increased intermetallic formation (Yeoh et al., 2004). Thus, appropriate rotational speed must be used to reduce any detrimental effects and generate joints with high quality.

2.5.3 Pressure

The axial pressure is applied to control the required power for Friction welding machine, the axial shortening of the components and the temperature gradient in the weld region. The specific axial pressure depends on the joint configuration, joint geometry and materials being joined (Ates et al., 2007). Pressure can be used to compensate for heat loss to a large components as in the case of bar to plate welds. Gowri (2007) and Kurt et al. (2011) also reported that applied pressure must be sufficiently high during the forging phase to keep the weld interfaces in close contact to avoid oxidation. Increasing the applied pressure at the end of the heating phase, can leads to improving the joint properties.

Mousavi and Kelishami (2008) discussed the effects of initial and final pressure on internal parameters. The initial pressure was applied during the welding time in which its values were increased to the final pressure during the braking time while the rotating speed decreases to zero. After cooling and applying the subsequent pressure, the process of recrystallization and growth occur that leads to the fine grain structure. It also implied that the initial pressure is an important parameter that helps with plasticity similar to rotational velocity.

2.6 Interface temperature

In friction welding, whether melting either occurs or not is still a controversial question (Maalekian, 2007). However, Nagappan (1970) reported that the melted phase may not occur or could be expelled before the melting began. They calculated the possibility of melting at the contacting surfaces of steel to AISI 1020 in their numerical and analytical transient temperature analysis of inertia welding. The experimental results showed that there was a distinguish difference in transient temperature behaviour between inertia and continuous drive friction welding. The temperature curve of inertia welding was much steeper than the continuous drive friction welding. They also noted that in both continuous drive and inertia welding, the interface temperature does not reach the melting point of the material when upsetting is taken into consideration and thus concluded that not melt had occurred.

Despite some reports from others experimental results which claimed melting at the interface, there were some strongly indicated that melting does not take place at the interface. The few researchers who reported melting at the interface, had based on their supposition on calculations, metallographic and temperature measurements. If any liquid is available near the solidus temperatures, it easily moves outwards before welding would occur. Furthermore, it should be emphasised that metallographic examination for solidification structures of friction welds may not be reliable to identify of liquids if liquated regions later solidify and undergo recrystallisation (Maalekian, 2007).

In addition, Wang (1975) indicated that metallurgical investigations do not support the existence of a liquid film at the interface, while torque measurements could not show any disruption that may be expected on account of a liquid interlayer. This pointed out that the temperature at the rubbing surface was below the melting temperature of the materials, as reported by Nagappan (1970).

2.7 Heat generation

Practically it has been recognised that the heat generation at the rubbing interface is not uniform. Accordingly, the uneven heating distribution at the interface generates with an increase near the centre towards the surface of welded components. Because the outer surfaces of the parts are in contact with the surrounding air, the temperature of those places will not reach the maximum value. According to the uneven temperature distribution, the

thickness of the heat affected zone (HAZ) becomes thicker from the centre to the periphery (Maalekian, 2007).

Sahin et al. (1996) have concluded that the temperature at the centre of the interface plane was less than at the mid-radius and surface. This was attributed to the heat generation which was relatively smaller at the centre. On the other hand, the temperature at the mid-radius of the interface was slightly less than the temperature at the surface due to the convection effect which was caused from the rotational motion of the weld parts.

In addition, Sahin et al. (1998) study revealed that the temperature of weld reaches its maximum value far from the centre but not at the free surface and the heat-transfer coefficient at the interface determines the distance of the location of this maximum from the surface.

In summary, it should be mentioned here that the variation of temperature at the interface in the radial direction plays an important role in the development of the HAZ, which subsequently, influences the quality of the weld. Owing to the difficulty in accurately measuring the temperature near the weld interface during friction welding, it requires thermocouples that are carefully attach and position within drilled holes away from the specimen surface. Due to the upset, the thermocouples moves with respect to the rubbing surface during welding, and usually the determination of the position of the thermocouples with time is difficult (Maalekian, 2007).

2.8 Structure of the heat affected zone (HAZ)

Some researchers had investigated the existence of diffusion layer in friction welding. The rubbing action, mating the surfaces on one another is due to the molecular and mechanical action. The molecular action is generated by a result of the diffusion molecular to one another while the mechanical action is a result of the rubbing two surfaces together. It has been concluded that diffusion is a primary mechanism contributing to friction welding. This is created by the parallel relative rotation and applied normal pressure (Maalekian, 2007).

Metallographic investigation of weld and HAZ zone for different materials has been studied. As shown in Figure 2.2, generally, the HAZ divided into different reaction zones (Lin et al., 1999; Özdemir et al., 2007; Sathiya et al., 2008; Ahmad Fauzi et al., 2010; Uday and Ahmad Fauzi, 2013).

(i) Full plastic deformed zone (FPDZ). The most microstructural changes occur in this region due to the frictional heat at the interface. Increasing temperature at the interface leads to the considerable plastic deformation which causing dynamic recrystallization and result in grain refinement.

(ii) Deformed zone (DZ). In this region, the temperature, strain rate as well as amount of plastic deformation are lower than zone (i). The microstructure becomes coarser due to the reduction in strain rate.

(iii) Undeformed zone or unaffected zone (UZ). Depending on the maximum temperature in this area, the material may undergo phase transformation, but plastic deformation does not occur. Grain growth may occur in this zone.

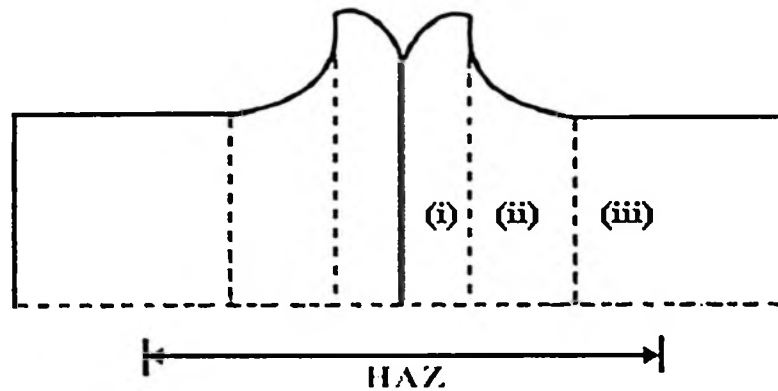


Figure 2.2: Schematic illustration of the different regions in the HAZ of friction welded specimens; (i) full plastic deformed zone (FPDZ); (ii) deformed zone (DZ); (iii) undeformed zone (UZ) (Ahmad Fauzi et al., 2010)

2.9 Classification of friction welding process

Welding process is a versatile and extensive technique for joining either similar or different (dissimilar) compositions. Mainly, there are five types of friction welding: rotary, linear, orbital, radial and friction stir welding (Uday, 2013). Rotary friction welding and stir friction welding are discussed as they are related to this study.

2.9.1 Rotary friction welding

Since the rotary friction welding (RFW) introduced during the Second World War, it emerged as the most common type of solid-state welding

processes where it was widely used by various industries for similar and dissimilar materials (Maalekian, 2007; Kurt et al., 2011; Davari et al., 2011). The basic principle of (RFW) is shown schematically in Figure 2.3.

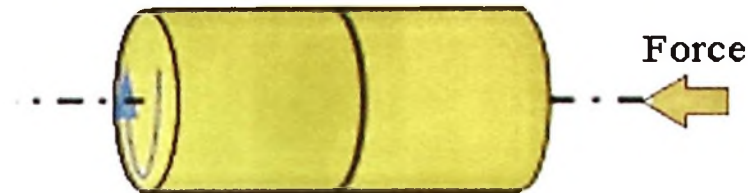


Figure 2.3: Schematic representation of the rotary manner

According to the method in which rotational energy is converted into frictional heat, rotary friction welding is divided into two basic types; the first one is known as direct drive or continuous drive friction welding (CDFW) and the second type is called inertia drive friction welding or stored energy. CDFW has been used since the 1940s. It provides constant energy from a source for any desired duration. On the other hand, IFW was developed in the early 1960s, which required welding energy that was provided by stored kinetic energy in a rotating flywheel (Davari et al., 2011).

1. Continuous drive friction welding (CDFW)

In CDFW, one of the components is attached to a motor driven which rotated at a constant speed, while the other is held stationary. Then the components to be welded are moved together by applying the pressure and then friction forms by rubbing the two components and generate heat at the faying interface (Nicholas, 2003). When a predetermined weld time or

amount of upset takes place, the rotating components is stopped by its own resistance or application of a braking force, while the axial force maintained or increased until the weld has cooled (Maalekian, 2007). Figure 2.4 is the schematic diagram of CDFW while Figure 2.5 shows schematically the variation in the parameter for CDFW. For the CDFW, controlling parameters are rotating speed, initial pressure, secondary pressure, duration of forging stage, and total time of friction welding.

As shown in Figure 2.5, the process can be divided into three phases. After the start of the process (in the initial phase), the speed increases rapidly to a peak value. After that, in the second phase, friction speed remains constant, indicating that the process reaches a balance between strain rate hardening and temperature softening. Strain hardening, also known as Work hardening, is the strengthening of a metal by plastic deformation (Maalekian, 2007). This strengthening occurs because of dislocation movements and dislocation generation within the crystal structure of the material. Work hardening is a consequence of plastic deformation, a permanent change in shape. Temperature softening is the determination of the softening point for materials that have no definite melting point, such as plastics.

Forging takes place in the third phase, which starts at the time of braking. Friction force increased before the speed of rotation fall off to zero sharply (Maalekian, 2007).

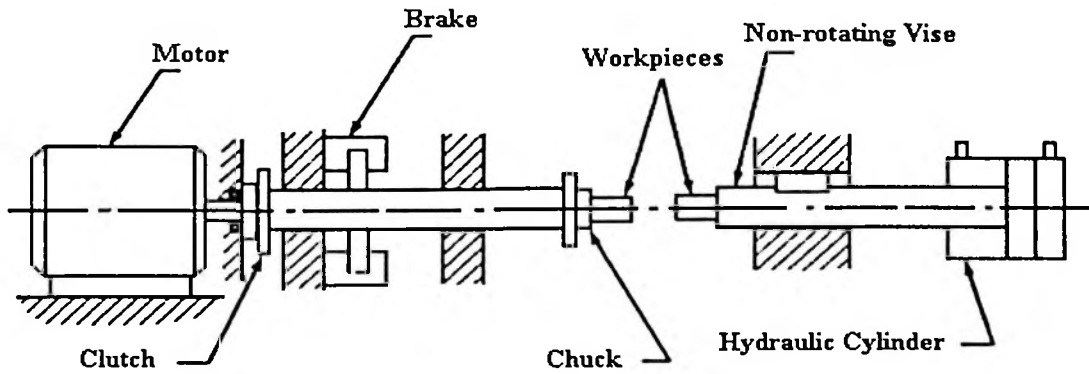


Figure 2.4: Schematic setup of a direct drive-welding machine (Davari et al., 2011)

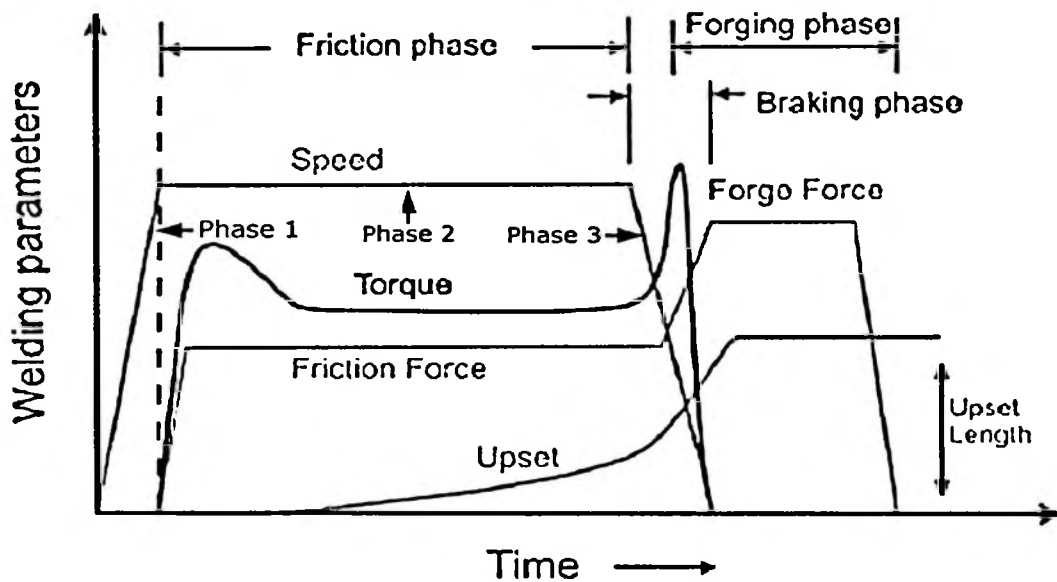


Figure 2.5: Schematic of parameter variations for direct drive friction welding process (Maalekian, 2007)

2. Inertia friction welding (IFW)

According to some researchers, in the inertia process, the rotating component is connected to a flywheel while the other is held stationary. Figure 2.6 shows the schematic setup of IFW machine. The flywheel is accelerated to a particular speed to store predetermined amount of energy. The drive motor is then disengaged and an axial force applied to force the

components together, in which components rub together and stored kinetic energy in the flywheel is consumed to generate heat at the faying interface. Eventually the speed of rotation decreased until rotation ceased and the axial force is maintained to consolidate the weld (Mortensen, 2001; Maalekian, 2007; Daus et al., 2007).

Figure 2.7 is the schematic of the variation in the parameter for IFW. In the case of the IFW, the process would be divided into two phases; in the first phase, the rotational speed increased gradually when it reached the peak and decreased steadily to zero in the second phase. The procedures explained for Continuous drive friction welding also occur in inertia friction welding. Except for the rotational speed, the changes of friction welding parameters with time are similar to those shown for Continuous drive friction welding.

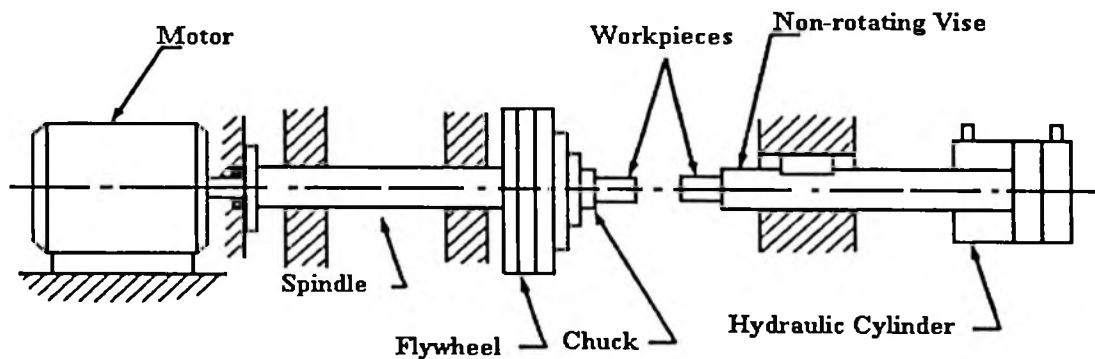


Figure 2.6: Schematic setup of an inertia-welding machine (Davari et al., 2011)

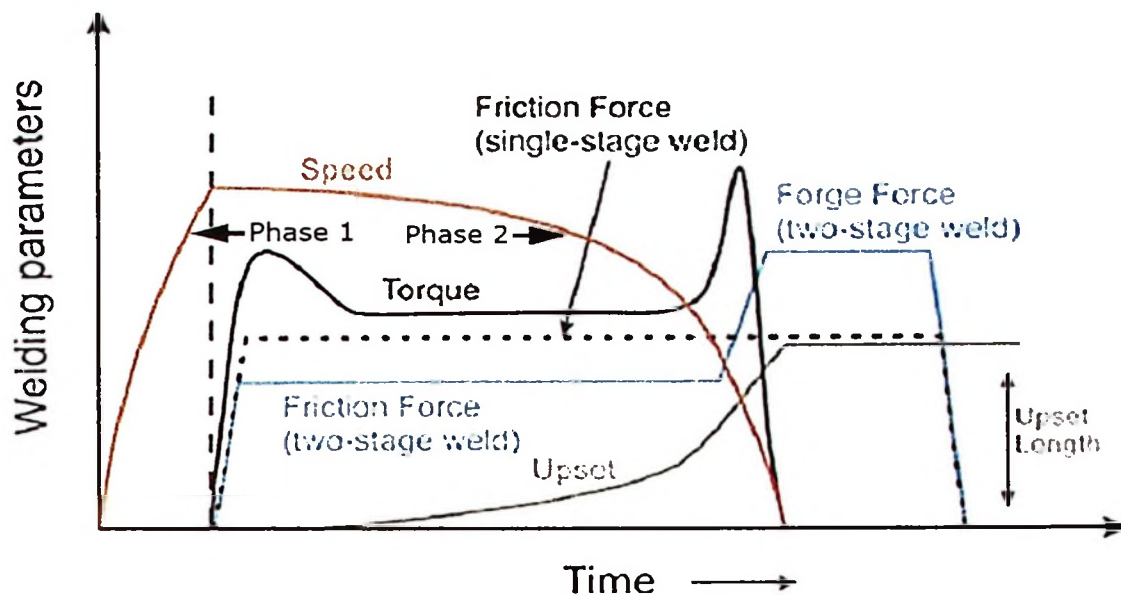


Figure 2.7: Schematic of parameter variations for inertia friction welding process (Maalekian, 2007)

The main differences of the two form of rotary friction welding are the variation of speed, force, and length of specimens (upset length) with time of welding for IFW and CDFW. It has been shown that welding time in IFW is shorter than in CDFW (Davari et al., 2011). Both processes (inertia and Continuous drive friction welding) produce excellent solid state bonds (Maalekian, 2007).

2.9.2 Friction stir welding

Friction Stir Welding (FSW), as a solid-state welding process which had create interest in researchers due to its outstanding weld properties and low environmental impact. It has been widely applied or investigated for joining of low melting temperature materials, such as aluminium alloys. Recently, there has been increasing research interest in high melting temperature materials, such as steel and titanium alloy (Zhao et al., 2013). FSW was used

for application where the original metal characteristics must remain unchanged as far as possible (Uday, 2013; Rustichelli, 2010; Huang et al., 2012).

Friction Stir Welding (FSW) method is a process of Advanced Welding Technology and was invented at The Welding Institute (TWI) of UK in 1991. It has been recognised that FSW is essentially a simple process of joining two materials (Mishra and Ma, 2005; Threadgill et al., 2009; Ma, 2008). The basic principles of FSW process are described excellently in a review by Ma (2008). As shown in Figure 2.8, a non-consumable rotating tool, specially designed with a pin and shoulder which is placed at the adjoining edges of sheets to be joined and then was made to traverse along the line of joint while the shoulder touches the sheets.

The heating is generated, principally due to the friction between the rotating tool and components and the two joining components, resulting in the plastic deformation of the material. Localized heating produces a softened zone of material around the pin and the combination of tool rotation and translation leads to movement of material from the front to the back of the pin. Hence, a welded joint formed in solid state (Mishra and Ma, 2005; Ma, 2008; Nandan et al., 2008; Threadgill et al., 2009; Gemme et al., 2011).

The friction Stir Welding (FSW) represents, in fact, an excellent technology that could be used for the design of aerospace and transport structures (Mishra and Ma, 2005; Gemme et al., 2011).